Optimal Trajectories of Spacecraft in the Expanse

Colin A. Miller[1]

[1] *Purdue University, West Lafayette, IN, 47906*

The Expanse is a science fiction series of novels and a television show that prides itself on keeping the physics in the show as realistic as possible with advances of technology the reader might expect to see humanity make in three hundred years. Assuming these technological advances are realistic, what falls into question is whether given the numbers of this new hardware, the physics of this story is accurate. This paper applies basic optimal control theory to this hardware in order to flush out whether the transit times between planets in the 24th century solar system are accurate and what exactly the optimal high-thrust, constant-burn trajectories are given these advancements. These paths will then be compared to those of more conventional technology including the classic Hohmann transfer and a low-thrust, constant burn trajectory, indicative of future electric propulsion engines. These regimes will be applied to two scenarios: an Earth to Moon trajectory and an Earth to Mars trajectory in order to compare transit times as well as the optimal control and trajectory.

Nomenclature

r = Radius from central body in kilometers

θ = Angle from x-axis typically in radians

u = Velocity in r-direction in kilometers per second

v = Velocity in θ-direction in kilometers per second

μ = Gravitational parameter of central body in kilometers squared per second squared

λ_r = Radius co-state

λ_θ = Angle co-state

λ_u = r-velocity co-state

λ_v = θ-velocity co-state

t = Time in seconds

I. Introduction

Set in the middle of the 24th century, the Expanse is a story imagining the future of humanity without too much suspension of disbelief. The only real advancements humanity has made are in technologies, the roots of which we already see in the current day. The largest technological advancement shown by this point is the Epstein drive, an ultra-efficient nuclear fusion reactor that produces immense amounts of thrust from very little mass for long periods of time. This radical new engine design enables faster and easier transport of goods and people around the solar system, allowing humanity to go from barely a two planet species to expanding onto the moons of Jupiter and Saturn, as well as having research facilities as far out as Neptune. Unlike most science fiction stories, humanity is not out exploring the galaxy with faster-than-light travel in the Expanse but is instead limited by the speed of their spacecraft which are still restricted to only current conventional physics. To quote the first novel in the series, Leviathan Wakes, "The Epstein Drive hadn't given humanity the stars, but it had delivered the planets." [3]

Rarely does the story give any exact figures on how long any of the spacecraft take to get to any of their destinations, however there are rough orders of magnitude. In general it is stated that traveling between planets in the inner solar system takes between days and weeks, depending on the orientation of the heavenly bodies, and will take weeks or months to go out to the outer solar system. The story also states that in general these ships cruise around at 30% Earth gravity or 0.3G. Given these rough numbers, this paper will explore how accurate these travel times are to both the Moon, hereby referred to as Luna, and Mars and will compare the optimal travel times and trajectories to those of of more conventional space travel. Assuming that far-future refers to the time period of the Expanse, near-future will refer to 50 to 100 years in the future. The conventional option for space travel in this paper is a standard two-burn trajectory, like those seen in the Apollo missions and continue to be used today. The near-future option is a low-thrust next generation ion drive, capable of outputting 20N of thrust. The far-future option will be the Epstein drive capable of continuous 0.3G burns for weeks or months on end.

II. Analysis

A. Dynamics

Firstly, the process equations must be defined, otherwise known as the equations of motion. It is here where the assumptions come into play. Newton's law of gravitation is the primary equation of motion to be dealt with. In cartesian coordinates this equation is:

$$a_g = \frac{\mu}{\sqrt{x^2 + y^2 + z^2}}[\boldsymbol{x}, \boldsymbol{y}, \boldsymbol{z}]$$

Where a_g is the acceleration due to gravity, μ is the product of the attracting body's mass and

Newton's constant, and x, y, and z are the cartesian coordinates of the orbiting body with respect to the attracting body. With the notable exception of Pluto, many of the celestial bodies in the solar system orbit the Sun in similar planes, thereby allowing the exclusion of one physical dimension in the analysis of the Earth to Mars trajectory. For the Low Earth Orbit (LEO) to Luna trajectory, it is also assumed that the initial orbit is coplanar to that of Luna's. Given these assumptions, a switch into cylindrical coordinates will prove fortuitous for the simplification of this spacecraft's equations of motion where the axes of this two dimensional plane are $\hat{r}$ and $\hat{\theta}$ and the velocities in these two dimensions are u and v, repectively. Thus the equations of motion are now:

$$\dot{r} = u$$

$$\dot{\theta} = \frac{v}{r}$$

$$\dot{u} = \frac{v^2}{r} - \frac{\mu}{r^2}$$

$$\dot{v} = -\frac{uv}{r}$$

These equations only define the motion of a simple orbiting body and do not take into account any other forces that may be exerted on the spacecraft. For this analysis the only other force of interest is the thrust produced by the spacecraft itself, thus all other gravity fields and orbital perturbations are assumed to be negligible. This thrust is described in the following equations:

$$T_\theta = T * cos(\alpha) \tag{1}$$

$$T_r = T * sin(\alpha) \tag{2}$$

Since these equations are defined in the $\hat{r} - \hat{\theta}$ frame, they can simply be added to the gravitational acceleration equations to give the full equations of motion:

$$\dot{r} = u \tag{3}$$

$$\dot{\theta} = \frac{v}{r} \tag{4}$$

$$\dot{u} = \frac{v^2}{r} - \frac{\mu}{r^2} + \frac{T}{m(t)} \sin\alpha \tag{5}$$

$$\dot{v} = -\frac{uv}{r} + \frac{T}{m(t)} \cos\alpha \tag{6}$$

Where the mass at any given time is given by:

$$m(t) = m_0 - |\dot{m}|t \tag{7}$$

It is important to note some assumptions for the different trajectories in this paper. Firstly, for the Hohmann transfer or Lambert transfer arc to both Luna and Mars, the burns are of such a relatively short duration that the change in mass may be treated as instantaneous and can be found for any given delta-V via the Tsiolkovsky rocket equation:

$$\Delta V = g_0 I_{sp} \ln \frac{m_{t_0}}{m_{t_f}} \tag{8}$$

Secondly, given the advanced nature of the propulsion system in the far-future case, and that it is incredibly efficient with its expulsion of mass, the mass of the spacecraft is assumed to be constant over the trajectory. Thus allowing the thrust over mass term to reduce to an acceleration, which in the novels is stated to typically be 0.3G. Lastly, this means that for only the near-future scenario takes into account a constantly changing thrust.

The last thing to be done is to scale these equations so that they are close to unity. Despite not having any physical significance, this allows for better accuracy when solving numerically as the computer will not have to truncate as many decimal places thereby reducing accuracy. All of these scaled terms will be denoted via a "bar" notation.

$$\bar{r} = \frac{r}{r_0} \tag{9}$$

$$\bar{v} = \frac{v}{v_0} \tag{10}$$

$$\bar{u} = \frac{u}{u_0} \tag{11}$$

$$\bar{T} = \frac{T t_f}{v_0} \tag{12}$$

A term, η will also be used for further simplification:

$$\eta = \frac{v_0 t_f}{r_0} \tag{13}$$

Going further with this in order to gain a term that is explicitly depending upon the gravitational parameter μ:

$$v_0 = \sqrt{\frac{\mu}{r_0}} \tag{14}$$

All further nondimensionalization is done to eliminate time and put everything in terms of a

nondimensional time, τ:

$$\tau = \frac{t}{t_f} \tag{15}$$

This reduces all equations of motion down to:

$$\frac{d\bar{r}}{d\tau} = \bar{u}\eta \tag{16}$$

$$\frac{d\theta}{d\tau} = \frac{\bar{v}\eta}{\bar{r}} \tag{17}$$

$$\frac{d\bar{u}}{d\tau} = \frac{\bar{v}^2\eta}{\bar{r}} - \frac{\eta}{\bar{r}^2} - \frac{\bar{T}}{m(\tau)} * \sin\alpha \tag{18}$$

$$\frac{d\bar{v}}{d\tau} = \frac{-\bar{u}\bar{v}\eta}{\bar{r}} - \frac{\bar{T}}{m(\tau)} * \cos\alpha \tag{19}$$

Where:

$$m(\tau) = m_0 - |\dot{m}|\tau t_f \tag{20}$$

This concludes the derivation of the equations of motion, however the α terms remain unknown and are currently unaccounted for in these equations of motion. This control is solved for using optimal control theory in the next section.

B. Optimal Control Theory

Finding the optimal trajectory or optimal control scheme is often anything but trivial and requires the derivation of equations of motion along with their co-states in order to analyze and solve a cost function. In the case of the minimum-time trajectory this cost function is the time, thus to optimize the trajectory to get the minimum time to travel to the destination the minimum of the travel time is desired. This is formulated in multiple ways according to different authors in the past:

$$Mayer : MinJ = t_f$$

$$Lagrange : MinJ = \int_0^{t_f} dt$$

$$Bolza : MinJ = \frac{1}{2}t_f + \frac{1}{2}\int_0^{tf} dt$$

Given these different formulations of the minimum time problem, the one most applicable to this problem is that of Mayer though all of the formulations are interchangeable.

The ideal formulation of this optimal control problem would be set up as follows: the state of the departure celestial body is known so its position and velocity becomes the initial conditions and the state of the destination celestial body is also known so its position and velocity become the final conditions. The focus is then to minimize the time of flight between these two boundary conditions. Despite this being ideal and seemingly straightforward, as noted in Longuski, Guzman, and Prussing (p. 235) there are computational difficulties preventing an accurate solution of this problem, thus the formulation is switched to a maximal radius problem. In this formulation, the initial conditions remain the same while the final conditions change slightly. The solver aims for only a circular orbit at the highest possible radius before running out of fuel. In the constant mass case, this would run continuously until the death of the computer, or more likely, the programmer is at wit's end. Thus a stopping condition is implemented when the final radius reaches the desired radius. The clear limitations here are that this solver can only take into account the radius of the target celestial body and not the location of the body in its orbit. This severely restricts the trajectories of the spacecraft in any real-world applications to only the times when the departure point is aligned correctly. However this is a similar drawback to that of the classical Hohmann transfer where the arrival and departure points must be exactly opposite each other.

Despite these limitations, the development of the rest of the process equations follows most other basic optimization problems. Letting x denote the state of a system and u denote the control of that system where H is the Hamiltonian, the co-state derivatives may be derived as such:

$$H = L + \lambda_x \dot{x} \tag{21}$$

$$\dot{\lambda_x} = -\frac{dH}{dx} = -H_x^* \tag{22}$$

$$\frac{dH}{du} = H_u^* = 0 \tag{23}$$

Additionally the fixed starting time version of the transversality condition as given by the the Euler-Lagrange theorem is:

$$H_f dt_f - \lambda_f^T dx_f + d\phi = 0 \tag{24}$$

To begin the optimal control theory analysis, the Hamiltonian is derived for this specific problem.

Here, there is no contributing "L" term, thus the Hamiltonian consists only of the sum of the products of the co-states with their respective process equations.

$$H = \lambda_{\bar{r}} * \frac{d\bar{r}}{d\tau} + \lambda_{\theta} * \frac{d\theta}{d\tau} + \lambda_{\bar{u}} * \frac{d\bar{u}}{d\tau} + \lambda_{\bar{v}} * \frac{d\bar{v}}{d\tau} \tag{25}$$

Or more explicitly:

$$H = \lambda_{\bar{r}} * [\bar{u}\eta] + \lambda_{\theta} * [\frac{\bar{v}\eta}{\bar{r}}] + \lambda_{\bar{u}} * [\frac{\bar{v}^2\eta}{\bar{r}} - \frac{\eta}{\bar{r}^2} - \frac{\bar{T}}{m(\tau)} * \sin\alpha] + \lambda_{\bar{v}} * [\frac{-\bar{u}\bar{v}\eta}{\bar{r}} - \frac{\bar{T}}{m(\tau)} * \cos\alpha] \tag{26}$$

This procedure seemingly brings the count of unknown variables up to eight despite only having four equations with which to solve for those unknown variables. However it is these variables with which a solution for the control will be obtained via the other tenants of the Euler-Lagrange theorem.

Firstly the process equations for the new unknowns may be found making use of the first result of the Euler-Lagrange theorem given by equation $:

$$\frac{d\lambda_{\bar{r}}}{d\tau} = -\frac{dH}{dr} = \lambda_{\bar{u}} * [\frac{\bar{v}^2\eta}{\bar{r}^2} - \frac{2\eta}{\bar{r}^3}] - \lambda_{\bar{v}} * [\frac{-\bar{u}\bar{v}\eta}{\bar{r}^2}] + \lambda_{\theta} * [\frac{\bar{v}\eta}{\bar{r}^2}] \tag{27}$$

$$\frac{d\lambda_{\theta}}{d\tau} = -\frac{dH}{d\theta} = 0 \tag{28}$$

$$\frac{d\lambda_{\bar{u}}}{d\tau} = -\frac{dH}{d\bar{u}} = -\lambda_{\bar{r}}\eta + \lambda_{\bar{v}}\frac{\bar{v}}{\bar{r}} \tag{29}$$

$$\frac{d\lambda_{\bar{v}}}{d\tau} = -\frac{dH}{d\bar{v}} = -\lambda_{\bar{u}}\frac{2\bar{v}\eta}{\bar{r}} + \lambda_{\bar{v}}\frac{\bar{u}\eta}{\bar{r}} - \lambda_{\theta}\frac{\eta}{\bar{r}} \tag{30}$$

Secondly, in order to eliminate the α terms from the equations of motions, the second tenant of the Euler-Lagrange theorem comes into play. It states that the derivative of the optimal Hamiltonian with respect to the control u is zero:

$$H_u^* = 0 = \lambda_{\bar{u}} * \frac{\bar{T}}{m(\tau)}\cos\alpha - \lambda_{\bar{v}} * \frac{\bar{T}}{m(\tau)}\sin\alpha \tag{31}$$

Simplifying and rearranging:

$$\tan\alpha = \frac{\lambda_{\bar{u}}}{\lambda_{\bar{v}}} \tag{32}$$

Geometrically, this equation may be thought of as defining a right triangle where the two legs are defined by $\lambda_{\bar{u}}$ and $\lambda_{\bar{v}}$ thus the hypoteneuse may be defined as $\sqrt{\lambda_{\bar{u}}^2 + \lambda_{\bar{v}}^2}$. This directly allows definitions of the α terms as follows:

$$\sin\alpha = \frac{\lambda_{\bar{u}}}{\sqrt{\lambda_{\bar{u}}^2 + \lambda_{\bar{v}}^2}} \tag{33}$$

$$\cos\alpha = \frac{\lambda_{\bar{v}}}{\sqrt{\lambda_{\bar{u}}^2 + \lambda_{\bar{v}}^2}} \tag{34}$$

There is some sign ambiguity for these definitions however for the purpose of this problem and given that the goal is to maximize the final radius of the spacecraft, both of these equations will be left as positive.

Lastly in the derivation of the process equations, two things must be found: the final value of the Hamiltonian and the value of the second co-state equation λ_θ. It was found earlier that:

$$\frac{d\lambda_\theta}{d\tau} = 0 \tag{35}$$

Which implies that

$$\lambda_\theta = constant \tag{36}$$

In order to solve for this constant, the last result of the Euler-Lagrange theorem comes into play, the transversality condition:

$$H_f dt_f - \lambda_f^T dx_f + d\phi = 0 \tag{37}$$

Which is is subject to the boundary conditions $d\Psi = 0$. Substituting in the terms related to the constant thrust problem:

$$-\lambda_{\bar{r_f}} d\bar{r_f} - \lambda_{\bar{v_f}} d\bar{v_f} - \lambda_{\theta_f} d\theta_f + dr_f = 0 \tag{38}$$

Where all other final terms are not free to change and therefore reduce to zero in this formulation. It is also known that:

$$d\Psi_1 = dv_f + \frac{1}{2}\sqrt{\frac{\mu}{r_f^3}} dr_f = 0 \tag{39}$$

Or:

$$dv_f = -\frac{1}{2}\sqrt{\frac{\mu}{r_f^3}} dr_f \tag{40}$$

Thus substitution leads to:

$$1 - \lambda_{\bar{r_f}} + \frac{1}{2}\lambda_{\bar{v_f}}\sqrt{\frac{1}{\bar{r_f}^3}} = 0 \tag{41}$$

And:

$$\lambda_{\theta_f} = 0; \tag{42}$$

Since the second co-state equation has been shown to be constant with respect to time and it is known that its final value is zero, it can be concluded that at all times:

$$\lambda_\theta = 0; \tag{43}$$

Finally, the full set of process equations and boundary conditions may be defined for this problem: Boundary conditions for time:

$$\tau_0 = 0 \tag{44}$$

$$\tau_f = 1 \tag{45}$$

Boundary conditions for the state and co-states:

$$\bar{r_0} = 1 \tag{46}$$

$$\theta_0 = 0 \tag{47}$$

$$\bar{u_0} = 0 \tag{48}$$

$$\bar{v_0} = 1 \tag{49}$$

$$\bar{u_f} = 0 \tag{50}$$

$$\bar{v_f} = \sqrt{\frac{1}{\bar{r_f}}} \tag{51}$$

$$1 - \lambda_{\bar{r_f}} + \frac{1}{2}\lambda_{\bar{v_f}}\sqrt{\frac{1}{\bar{r_f}^3}} = 0 \tag{52}$$

$$\lambda_{\theta_f} = 0 \tag{53}$$

Process equations, substituting in the co-state formulations of control for the α terms:

$$\frac{d\bar{r}}{d\tau} = \bar{u}\eta \tag{54}$$

$$\frac{d\theta}{d\tau} = \frac{\bar{v}\eta}{\bar{r}} \tag{55}$$

$$\frac{d\bar{u}}{d\tau} = \frac{\bar{v}^2\eta}{\bar{r}} - \frac{\eta}{\bar{r}^2} - \frac{\bar{T}}{m(\tau)} * \frac{\lambda_{\bar{u}}}{\sqrt{\lambda_{\bar{u}}^2 + \lambda_{\bar{v}}^2}} \tag{56}$$

$$\frac{d\bar{v}}{d\tau} = \frac{-\bar{u}\bar{v}\eta}{\bar{r}} - \frac{\bar{T}}{m(\tau)} * \frac{\lambda_{\bar{v}}}{\sqrt{\lambda_{\bar{u}}^2 + \lambda_{\bar{v}}^2}} \tag{57}$$

$$\frac{d\lambda_{\bar{r}}}{d\tau} = \lambda_{\bar{u}} * [\frac{\bar{v}^2\eta}{\bar{r}^2} - \frac{2\eta}{\bar{r}^3}] - \lambda_{\bar{v}} * [\frac{-\bar{u}\bar{v}\eta}{\bar{r}^2}] + \lambda_\theta * [\frac{\bar{v}\eta}{\bar{r}^2}] \tag{58}$$

$$\frac{d\lambda_{\bar{u}}}{d\tau} = -\lambda_{\bar{r}}\eta + \lambda_{\bar{v}}\frac{\bar{v}}{\bar{r}} \tag{59}$$

$$\frac{d\lambda_{\bar{v}}}{d\tau} = -\lambda_{\bar{u}}\frac{2\bar{v}\eta}{\bar{r}} + \lambda_{\bar{v}}\frac{\bar{u}\eta}{\bar{r}} - \lambda_\theta\frac{\eta}{\bar{r}} \tag{60}$$

Where:

$$m(\tau) = m_0 - |\dot{m}|\tau t_f \tag{61}$$

The derivation of these boundary conditions and process equations is the same as in Longuski, Guzman, and Prussing[1] which also gives credit to Peter J. Edelman and Kshitij Mall. This derivation is included for this paper to be fully self-contained. In addition to exactly this formulation some modifications are made for the far-future case and the assumption of constant mass. For that problem the $\frac{\bar{T}}{m(\tau)}$ term is replaced by simply $\bar{a}$ where a is the constant acceleration of the spacecraft such that:

$$\bar{a} = \frac{at_f}{v_0} \tag{62}$$

Changing from a force to acceleration and neglecting to divide by mass in this problem still keeps the process equations dimensionless. The only change to the process equations is listed below:

$$\frac{d\bar{u}}{d\tau} = \frac{\bar{v}^2\eta}{\bar{r}} - \frac{\eta}{\bar{r}^2} - \bar{a} * \frac{\lambda_{\bar{u}}}{\sqrt{\lambda_{\bar{u}}^2 + \lambda_{\bar{v}}^2}} \tag{63}$$

$$\frac{d\bar{v}}{d\tau} = \frac{-\bar{u}\bar{v}\eta}{\bar{r}} - \bar{a} * \frac{\lambda_{\bar{v}}}{\sqrt{\lambda_{\bar{u}}^2 + \lambda_{\bar{v}}^2}} \tag{64}$$

In addition to this problem setup, it has been shown that the most fuel-efficient trajectory to get from one orbit to another co-planar orbit is the Hohmann transfer[2]. Just like the previous derivation was for the time-optimal trajectory, one may call the Hohmann transfer the fuel-optimal trajectory. This trajectory involves a specific orbital geometry where the initial position of the

spacecraft and the final position of the spacecraft are on opposites sides of the central attracting body, both the initial and final orbits are circular, and both orbits are in the same plane. Many conditions must be correct in order for this type of transfer to be used. Nevertheless, it serves as a classical comparison for many more modern or experimental trajectories in space as it has been used extensively by many of the space agencies around the globe. As there are many resources for the computation of such a trajectory, its derivation will be omitted from this paper.

III. Numerical Results

A. Covergence of Solutions

One common thread throughout all of numerical optimization seems to be the difficulty in getting any solution to converge and at times can make any optimization problem feel much more like an art than a science. The optimal time for constant thrust trajectories between celestial bodies is no different. A seemingly common tactic is described in Longuski, Guzman, and Prussing where instead of solving for the complete trajectory at the beginning, the time of flight, given by t_f in the formulation is gradually stepped up from a very small time representing a tiny fraction of the necessary trajectory. This short timespan in general leads to a greater likelihood of having the solution converge since it is not trying to solve over a very large distance for any given iteration. This solution is then used as the initial guess for the solution of the next iteration with a slightly higher time of flight. This procedure works exceptionally well for any trajectories within Earth's sphere of influence and was the primary method of getting a solution to converge when transversing the distance of LEO to Luna

This solution did not suffice for the Earth to Mars trajectory and required even more finesse. Many attempts were made to try to get this Sun-centered problem to converge and none seemed to work. Despite having the same spirit as the LEO to Luna problem, the main barrier to overcome was the vastly increased magnitude of the distances as well as the greatly increased gravitational parameter of the Sun. Of the various trials the primary parameters changed were the time step, by making t_f much smaller, slowly scaling up the destination radius until reaching that of Mars' semi-major axis, and even slowly scaling up the gravitational parameter of the central body to that of the Sun's. This was all to no avail where not even in the initial guess would converge.

The main difference between the LEO-Luna problem and the Earth-Mars problem is the magnitude of the attracting body's acceleration on the spacecraft, as given by the magnitude of Newton's equation:

$$F = -\frac{\mu}{r^2} \tag{65}$$

The key to getting any optimal trajectory to converge around the Sun, at least in this formulation of the problem, was to match this magnitude of gravity to that of one where the solution is known

to converge. In this case, the LEO-Luna problem converged without issue so all that was needed was to start the spacecraft in an orbit that would yield a similar gravitational acceleration. It turns out that at a 300 km altitude above Earth, the spacecraft would experience the same acceleration 4 million kilometers from the Sun. This trick allowed both the initial guess and the solution to converge for the Earth-Mars transit however the initial radius of such a solution would not match that of Earth's 150 million km.

To get the optimal trajectory of this solution to be that of an Earth to Mars transit, multiple steps had to be taken within the confines of the derived solution to this problem. Firstly, as with the Luna setup, the target radius had to be set, however instead of simply settig the orbital radius of Mars, the distance between the orbits of Earth and Mars was set. This is approximately 80 million km. This solution would provide a trajectory departing from around 4 million km from the Sun and arriving at a circular orbit 84 million km out. This was iterated over using via the same method described for the LEO-Luna problem. Once this solution was found, it was used as the initial guess starting at Earth's orbit and arriving at Mars' orbit. Again this was more accurately solved via iterating over the small time steps.

These methods provided accurate results for trajectories leaving from either LEO or Earth's orbit and arriving in the proximity of Luna's or Mars' orbit respectively. To get the tolerance of the final radius even closer to that of a target, a method is discussed in the next section to iteratively reduce the error.

B. Turning a Maximal Radius Problem into a Minimum Time Problem

The last issue to overcome in this optimization problem is that of reducing the final radius error to a small and controllable amount. Ideally the way to solve this would be by having an analytical relationship between the control variable for the solver, in this case t_f, and the output variable of interest, r_f. However this is not the case and is not even easily estimated. To be succinct, it is not known how changes in t_f change the values of r_f. Newton provided a simple way of doing so, needing only to calculate the value of the first derivative for the change in unknown variable with respect to that of the known[8]. Newton's method as can be seen in the context of the minimum time trajectory is seen below:

$$t_{f,i+1} = t_{f,i} - \frac{r_f(t_{f,i})}{r'_f(t_{f,i})} \tag{66}$$

Where $r'_f(t_{f,i})$ denotes the derivative of the final radius with respect to the input final time. The implementation of Newton's method requires slight changes to the input. The minor perturbations are denoted as t_f^+ and t_f^- where the original input value is t_f. Each of these will result in their own solution with their own values of the final radius, denoted r_f^+, r_f^-, and r_f respectively. The first derivative term is then:

$$r'_f(t_{f,i}) = \frac{r_f^+ - r_f^-}{t_f^+ - t_f^-} \tag{67}$$

This process may be repeated as many times as is desired for better and better accuracy but in general 3-5 iterations have seemed to be sufficient. It is also important to note that in order for this iteration to work, all values must be scaled back to their original dimensions.

C. Output

C..1 Earth to Moon

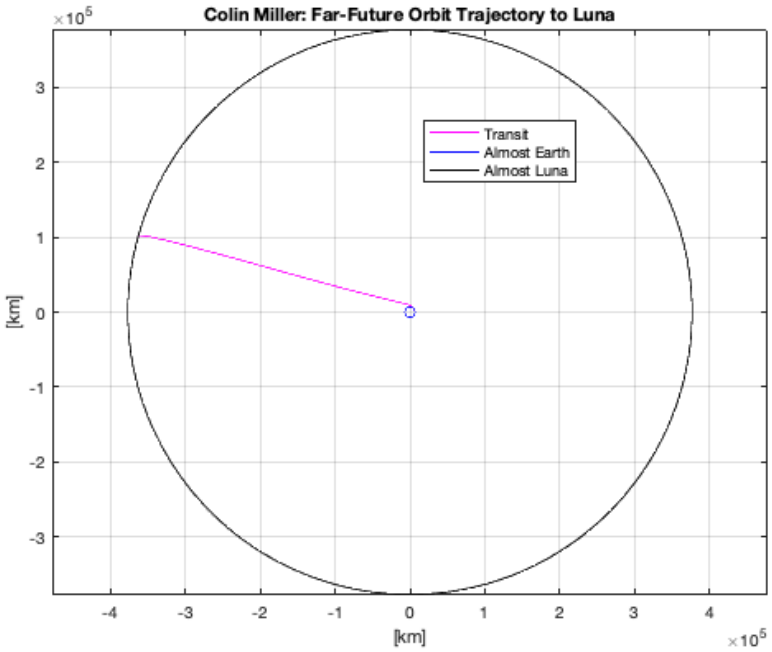

Figure 1: Far-future Earth to Luna trajectory as would be seen in the Expanse for the minimum time solution.

As depicted in the figure above, the minimum-time trajectory from LEO to Luna is seemingly a straight line directed toward Luna with only slight curves in departure and arrivel so as to match the orbital velocity of the corresponding body. There is a much larger curve in the departure from LEO due to the high gravitational pull of being so close to the Earth. This similar to how an escape trajectory is relatively curved when close to the attracting body but straightens out the further away the spacecraft gets, approaching a linear asymptote at an infinite distance. Because of the large amount of thrust, the spacecraft accelerates towards Luna for half of the journey and then

decelerates to match the orbital velocity of Luna for the other half. Essentially this high thrust in comparison to the gravitational pull of Earth allows for seeming linear motion in space, despite still being acted upon by gravity.

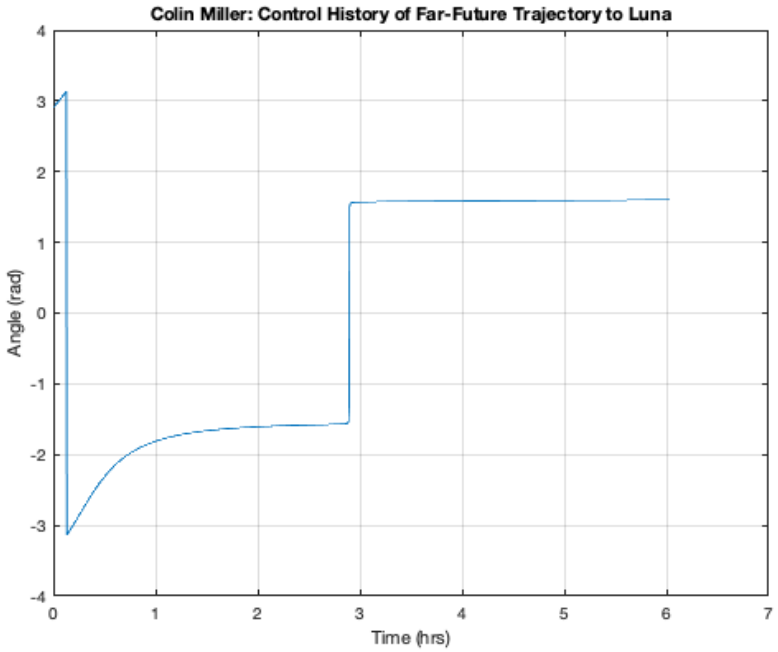

Figure 2: Far-future Earth to Luna trajectory control of a hypothetical spacecraft in the Expanse.

In the Expanse, there is a common maneuver referred to as a "flip and burn" which occurs when transiting between two places in the solar system, midway through the journey, and after a long acceleration towards the destination the ship is turned around and begins a burn in the opposite direction in order to decelerate before reaching the destination, and to match the destination's orbital velocity. This is seen prominently in the control history of the thrust direction where halfway through the transfer time, there is a jump of around 180 degrees. In addition to this there is what seems to be a jump in the very beginning. This is due to a wrapping issue where the functions used to calculate the control history only work on the interval [-360, 360] degrees. There is also a gradual increase in the steering angle at the beginning of the flight. This is because the spacecraft still is accelerating away from Earth to put itself on that seemingly linear trajectory. In the Expanse this is referred to as going "up the well" (James S. A. Corey p. 438).

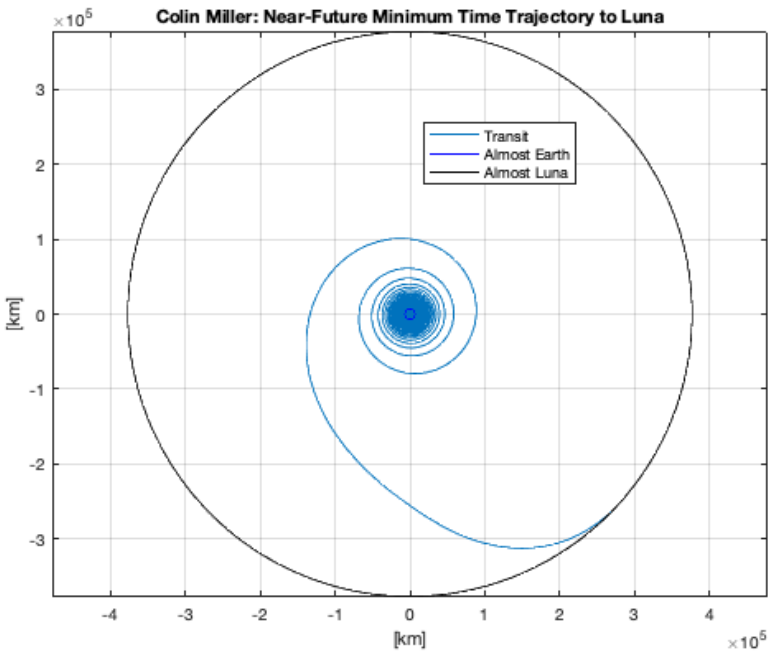

Figure 3: Near-future Earth to Luna trajectory with advanced electric propulsion delivering 20N of thrust.

Despite being another constant thrust scenario, the near-future electric propulsion engine used produces very different results from that of the high thrust far-future engine. Instead of traveling directly towards the destination the spacecraft spirals out from the departure orbit, continuing for many complete orbits around the Earth until eventually the spiral reaches the orbital radius of Luna. As will be discussed later, this trajectory takes significantly longer than both the far-future case as well as a simple Hohmann transfer. In essence this type of engine trades time of flight for fuel efficiency.

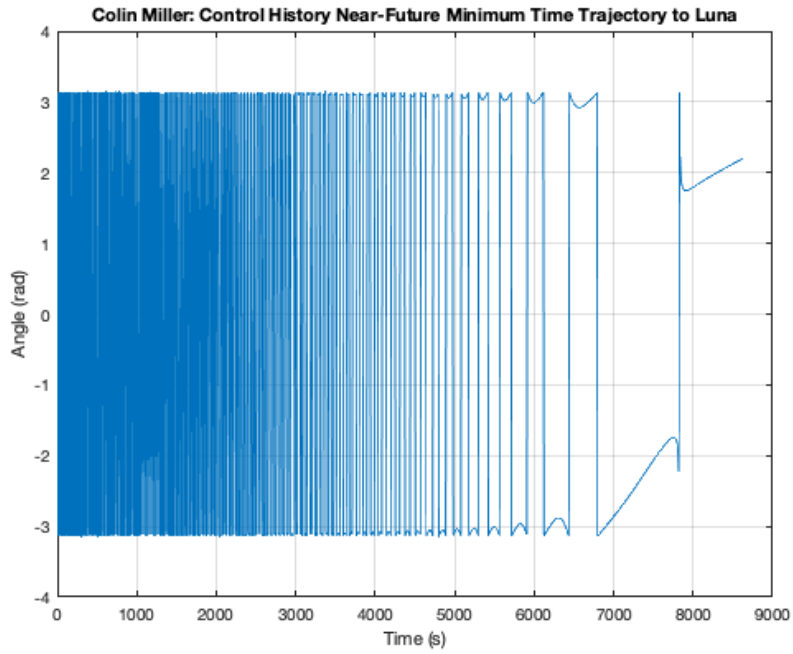

Figure 4: Near-future Earth to Luna trajectory control history with advanced electric propulsion delivering 20N of thrust.

The trend in control history for this low thrust transfer to Luna indicates that the switching of direction of thrust is timed according to the orbital period. Despite the wrapping issues jumping around the interval [-360, 360], the period of the changing control starts by being very short but gradually increases as the spacecraft proceeds away from Earth until it reaches Luna. In addition the trend on a per-orbit basis remains relatively the same despite the changing period length and appears to oscillate while slowly growing in magnitude over the entire trajectory. This behavior is likely due to a need to reduce the periapsis and extend the apoapsis as much as possible. With an extended apoapsis, the spacecraft is reaching its orbit out towards Luna more and more each orbit but by shrinking the periapsis, the spacecraft can make use of the Oberth effect where it is more efficient in terms of ΔV to increase the speed of the spacecraft where the speed is already the highest. The highest speed is at periapsis, thus engines are activated in the direction of v to increase speed at periapsis and extend the apoapsis, and then are turned towards $-v$ in order to minimize the periapsis in order to increase the speed at the next passage of periapsis. It is possible that the most efficient form of this maneuver would consist of piecewise continuous control, activating the engines only around periapsis and apoapsis, reducing the waste of fuel for the rest of each orbit, however this is beyond the current formulation of the problem.

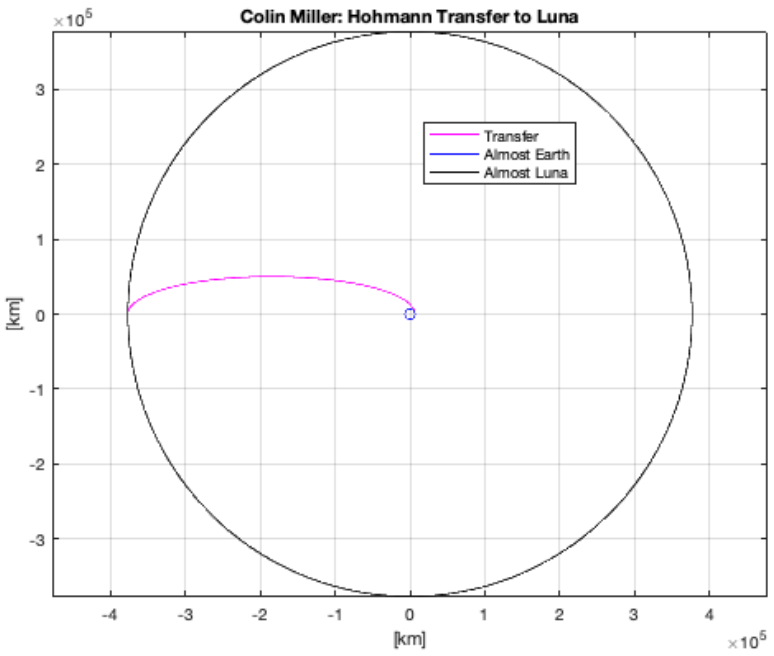

Figure 5: Earth to Luna trajectory using conventional technology for a Hohmann transfer.

Depicted above is a standard Hohmann transfer from Earth to Luna. This is not the trajectory that Apollo used and in fact it used a more expensive free-return trajectory; however, both types of transfers are the standard two-burn transfers that are used very commonly in mission design. What happens here is that in order to initiate a transfer, the spacecraft thrusts for a short period of time to raise its apoapsis to the radius of the targeted destination, so that the spacecraft will arrive at the destination upon reaching apoapsis. Then another burn is initiated in a Hohmann transfer in order to match the velocity and therefore circularize its orbit in order to arrive at its destination. Necessarily there must be a control history although none has been reported as the Hohmann transfer is already the optimal solution and this control history would appear to be a positive instantaneous spike at the beginning, undefined for the duration of the flight since the steering angle cannot be determined without thrust, then an instantaneous negative spike at the end.

C..2 Earth to Mars

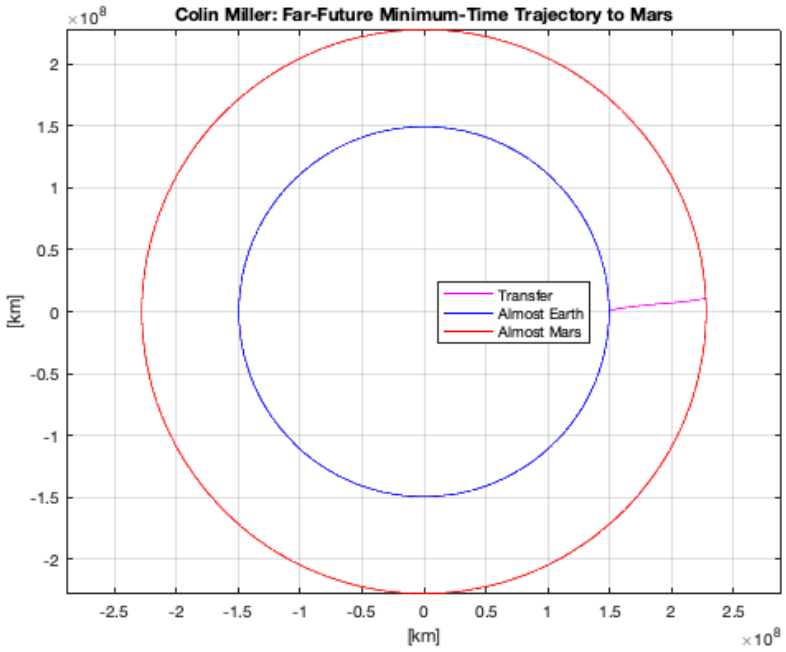

Figure 6: Far-future Earth to Mars trajectory as would be seen in the Expanse for the minimum time solution.

The inherent issues with the formulation of this optimization problem are clearly evident here. Since the only apparent final boundary conditions must be physical, the goal is only to reach the desired radius and to match the velocity of the destination at that radius. Thus there is no control over the location of the destination in this two dimensional problem. If there were, one of the final boundary conditions would contain information about θ_f, the angle where the destination, Mars here, is located at the end of the transfer. Since this does not exist, the optimal solution is only to achieve the desired orbital radius as quickly as possible, thus the spacecraft seems to accelerate radially outward from the Sun as fast as possible. A future formulation would take into account better location data of the departure and destination locations, allowing for travel at any geometry of Earth and Mars, rather than having to wait for a specific alignment of the planets as is the case here.

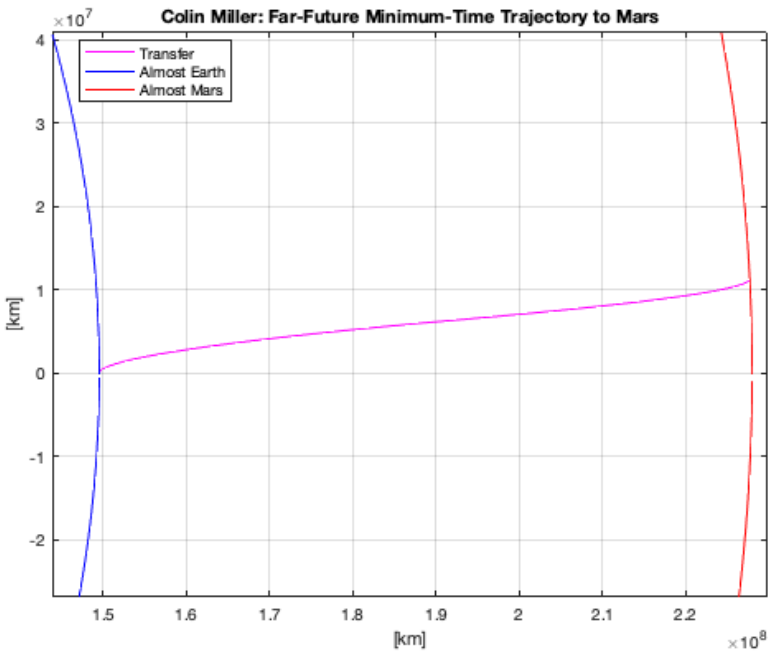

Figure 7: Far-future Earth to Mars trajectory close-up showing the departure and arrival trajectories more clearly.

A close-up view of the transfer trajectory itself is provided to show better detail of the departure and arrival behavior. Instead of being a simple linear trajectory between Earth and Mars, there are slight curves in departure and arrival. The curves appear because of the initial and final conditions specifying that the velocity of the spacecraft must match that of the planets. If instantaneous changes in velocity were allowed, the trajectory would look like two 90 degree turns, one in leaving Earth to go travel radially out from the Sun and one and then another to change from moving radially out to moving with the orbit of Mars. Instead the physical limitations on this far-future spacecraft become apparent despite it's efficient and high thrust engine, as the spacecraft gradually curves out from Earth and curves towards Mars, resulting in a slight "S" shaped trajectory.

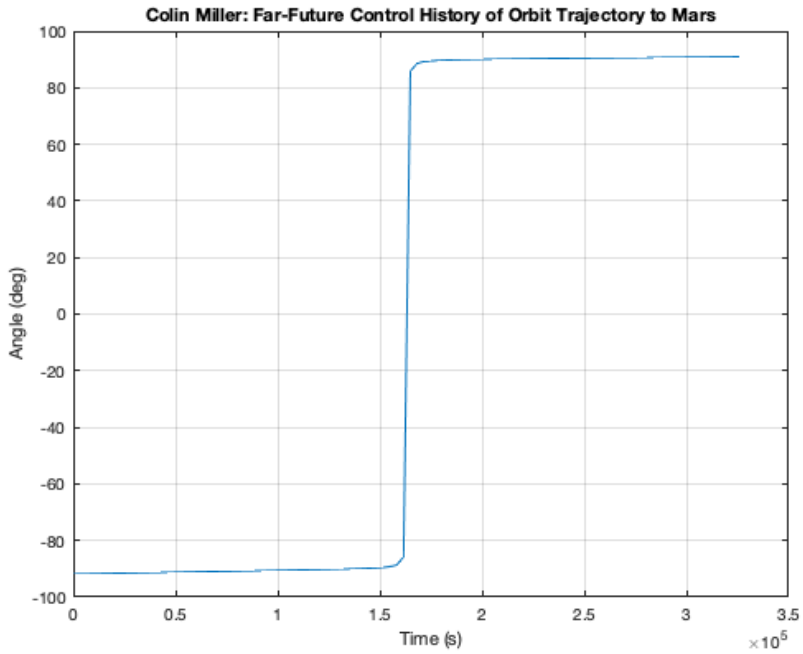

Figure 8: Far-future Earth to Mars trajectory control of a hypothetical spacecraft in the Expanse.

The "flip and burn" as described earlier becomes even clearer in the Earth to Mars transfer due to the much lower magnitude of gravitational acceleration on the spacecraft from being so far from the attracting body, the Sun, throughout the duration of its journey. This brings the behavior of the spacecraft much closer to that of linear motion between two points, similar to the problem of a moving bead on a wire where gravity acts more like a slight perturbation rather than a main force on the spacecraft. The effects of gravity can still be seen in the gradual incline of the steering angle over its relatively flat periods. This incline accounts for the slightly changing magnitude of gravity as the spacecraft gets further and further away from the Sun. The major change occurs at almost exactly midway through the flight when, in order to match the orbital velocities of Earth and Mars, the spacecraft switches from accelerating away from Earth to decelerating towards Mars. This flip is near instantaneous with respect to the total flight time and must occur as the spacecraft has to cancel out the momentum it gained in its outward acceleration. Additionally it must occur halfway through as the thrust is fixed throughout the journey with only the steering angle changing. Further investigations may involve changing thrust throughout the trajectory, however in the Expanse 0.3G is chosen as this is what humans living on Mars, the asteroid belt, and beyond are used to due to developing in low-G spin gravity over their lives, thus the thrust is limited by human physiology as described in the novels.

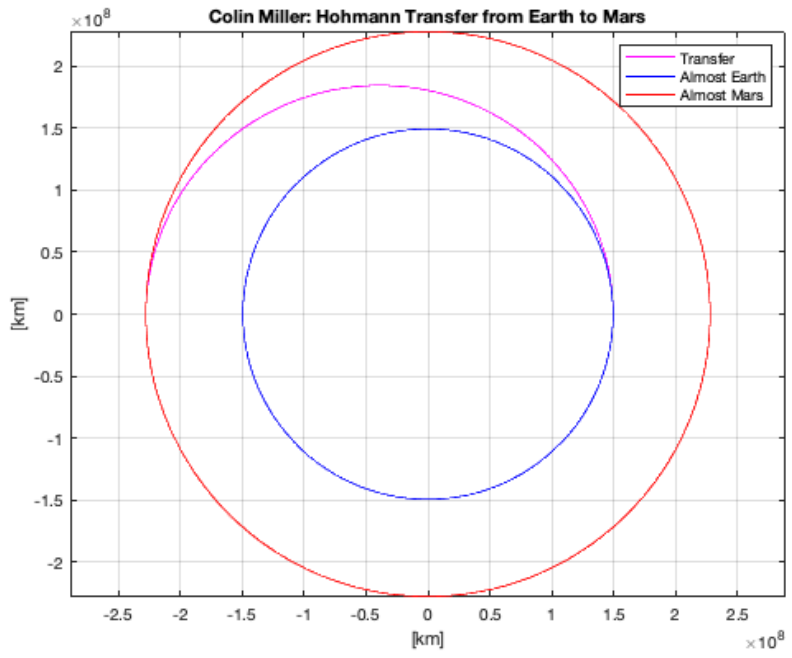

Figure 9: Earth to Mars trajectory with current technology using a Hohmann transfer.

For comparison, a classical Hohmann transfer is depicted, where Earth at departure and Mars at arrival are 180 degrees apart. The time of flight for this is around eight months or 243 days. This is more than that used in the typical transfers to Mars such as that of Perseverance where NASA lists its transfer as only taking 188[7] days. Despite this discrepancy, both two-burn transfers are relatively similar in geometry and show the large difference between conventional trajectories to Mars and the far-future minimum-time trajectory to Mars as would be seen in the Expanse.

Time Period	Transfer to Luna	Transfer to Mars
Current	4.842 days	8.5 months
Near-Future	31.60 days	N/A
Far-Future	6.036 hours	3.779 days

Table 1: Transfer times for the different technological eras between two celestial bodies of interest. The near-future or advanced electric propulsion scenario to Mars was omitted due to difficulty in convergence of an optimal solution.

IV. Conclusion

This project and the results of the paper met or exceeded expectations. The primary result that was sought was the relatively instantaneous turnaround in the steering angle, or as it is referred to in the Expanse, the "flip and burn." This was extremely evident in the control history of all of the far-future scenarios that would be representative of the Expanse and its ships.

1. Any spacecarft capable of sustained high-thrust throughout its transfer will not follow classical trajectories through the solar system.

2. Spacecraft capable of sustained high-thrust will have considerably reduced flight times as compared to more conventional spacecraft.

3. The characterization of control history is greatly impacted by the transit time and whether the spacecraft completes more than one full orbit during its transfer.

4. As the thrust and sustainability of spacecrafts' propulsion increase, their trajectory and control history more closely resemble that of free motion, with no forces acting upon the spacecraft other than the thrust.

5. In general the further away a spacecraft is from its attracting body, the less rapidly the spacecraft must alter its control.

6. If the technology were available for sustained high-thrust spacecraft, this would be the best solution for interplanetary travel. Until then crewed missions will likely benefit from the shorter travel times of the Hohmann transfer, however less time sensitive missions would likely benefit from the fuel efficiency of electric propulsion systems.

A. Future Work

1. Re-formulate optimization problem with control over not just r_f, u_f, and v_f but also θ_f thereby allowing for optimal trajectories around the solar system more independent of specific geometries of planets.

2. Pose another optimization problem with control over both steering angle and thrust.

3. Work to ensure convergence of the near-future, low-thrust scenario to Mars in order to better compare interplanetary minimum-time trajectories.

4. Extrapolate the solutions in full three-dimensional space to better reflect reality.

5. Change the u_0, v_0, u_f, and v_f boundary conditions to better reflect the orbital eccentricities of celestial bodies.

Appendix

This is only the code for the optimal far-future (high-thrust) constant-thrust to Mars scenario for the purpose of brevity. All other optimal formulations are some variations on this.

Main function:

```
%%%%%%%%%%%%%%%%%%%%%%%%%%%%%%%%%%%%%%%%%%%%%%%%%%%%%%%%%%%%%%%%%%%%%%%%%%%%%%%
% Maximal Orbit Raise to Reach Mars
% Based on Optimization and Aerospace Applications
%
% Uses bvp4c to solve maximal orbit raise from Earth to Mars
%
% Author: Jose J. Guzman, George E. Pollock, Peter J. Edelman
% Re-Created: Colin Miller
% Recreation Date: 11/13/2020
%%%%%%%%%%%%%%%%%%%%%%%%%%%%%%%%%%%%%%%%%%%%%%%%%%%%%%%%%%%%%%%%%%%%%%%%%%%%%%%

% Resetting everything
close all; clear all; clc;

% Importing constants for the solar system
AAE450_ConstantInit;

% Define parameters

r0 = 4e6;       % Beginning radius from Sun in km
mu = Sun.GM;   % Gravitational parameter of Sun
g0 = 9.80665;        % Standard gravity on Earth
v0 = sqrt(mu/r0);
u0 = 0;
gfrac = 0.3;
targetRadDest = Mars.SMA;
targetRadDepa = Earth.SMA;

global m0 mdot vbar0 ubar0 rbar0 theta0 eta accbar ubarf tf Hf nu thetaf
vbar0 = v0/v0;
ubar0 = u0/v0;
rbar0 = r0/r0;
theta0 = 0;
```

```
thetaf = pi/2;
nu = 1;

numdays = 0.1;

ubarf = 0.1;
tf = numdays*86400;       % Final time in seconds
Hf = -1;

eta = v0*tf/r0;
accbar = gfrac*g0*tf/v0/1000;

% Initial Guesses

% Initial Time
t0 = 0;
lambda20 = 0;
lambda30 = -1;
lambda40 = 0;

% Defining initial guess array
yinit = [rbar0, theta0, ubar0, vbar0, lambda20, lambda30, lambda40];

% Discretized number of points
Nt = 100;

tau = linspace(0, 1, Nt)'; % non-dimensional time vector

% Initial guess of solution
solinit = bvpinit(tau, yinit);

option=bvpset('Nmax',500000);

% Solution
sol = bvp4c(@max_rad_orbit_odes, @max_rad_orbit_bcs, solinit, option);

% Evaluate solution at all times
z = deval(sol, tau);
```

```
numdays = 0.2;

ubarf = 0;
tf = numdays*86400;       % Final time in seconds
Hf = -1;

eta = v0*tf/r0;
accbar = gfrac*g0*tf/v0/1000;

% Convert dimensionless time to dimensional time
time = t0 + tau.*(tf-t0);
numdays = 0.1;


% Begin basic convergence iteration loop
while ((z(1, end)*r0 - z(1, 1)*r0) < (targetRadDest - targetRadDepa))
    tf = 86400*numdays;
    accbar = gfrac*g0*tf/v0/1000;
    eta = v0*tf/r0;
    solinit.y = z;
    solinit.x = tau;
    sol = bvp4c(@max_rad_orbit_odes, @max_rad_orbit_bcs, solinit, option);
    z = deval(sol, tau);
    numdays = numdays + 0.1;
end

% Save all solution information
solinit.y = z;
solinit.x = tau;

% Reset using solution for Earth to Mars trajectory
r0 = targetRadDepa;
v0 = sqrt(mu/r0);
vbar0 = v0/v0;
ubar0 = u0/v0;
rbar0 = r0/r0;
theta0 = 0;
```

```
sol = bvp4c(@max_rad_orbit_odes, @max_rad_orbit_bcs, solinit, option);
z = deval(sol, tau);

% Discretized number of points
Nt = 100;

tau = linspace(0, 1, Nt)'; % non-dimensional time vector

% Vector of information saved to start Newton iteration
itnum = 1;
tfvec(itnum) = tf;
rfvec(itnum) = z(1, end)*r0;

% Begin Earth-Mars trajectory loop
while z(1, end)*r0 > targetRadDest
    itnum = itnum + 1;
    tf = 86400*numdays;
    accbar = gfrac*g0*tf/v0/1000;
    eta = v0*tf/r0;
    solinit.y = z;
    solinit.x = tau;
    sol = bvp4c(@max_rad_orbit_odes, @max_rad_orbit_bcs, solinit, option);
    z = deval(sol, tau);
    numdays = numdays - 0.02;
    numdaysvec(itnum) = numdays;
    rfvec(itnum) = z(1, end)*r0;
%    z(1, end)*r0
end

% Save information for next iteration
solinit.y = z;
solinit.x = tau;

% Starting Newton iteration
rNewt = rfvec(end-1)*r0;
rNewtp = rfvec(end)*r0;
rNewtm = rfvec(end-2)*r0;
numdaysNewt = numdaysvec(end-1);
```

```
numdaysNewtp = numdaysvec(end);
numdaysNewtm = numdaysvec(end-2);
fNewt = rNewt - Moon.SMA;
fpNewt = (rNewtp - rNewtm)/(numdaysNewtp - numdaysNewtm);
numdays = numdaysNewt - fNewt/fpNewt;

clear rvec numdaysvec
while abs(rNewt - targetRadDest) > 100
    % Get the incremented and decremented time values for Newton scheme
    numdaysp = numdays + 0.05*(numdaysNewtp - numdaysNewtm);
    numdaysm = numdays - 0.05*(numdaysNewtp - numdaysNewtm);

    % Do middle data for Newton method
    tf = 86400*numdays;
    accbar = gfrac*g0*tf/v0/1000;
    eta = v0*tf/r0;
    sol = bvp4c(@max_rad_orbit_odes, @max_rad_orbit_bcs, solinit, option);
    z = deval(sol, tau);

    % Do minus data for Newton method
    tf = 86400*numdaysm;
    accbar = gfrac*g0*tf/v0/1000;
    eta = v0*tf/r0;
    sol = bvp4c(@max_rad_orbit_odes, @max_rad_orbit_bcs, solinit, option);
    zm = deval(sol, tau);

    % Do plus data for Newton method
    tf = 86400*numdaysp;
    accbar = gfrac*g0*tf/v0/1000;
    eta = v0*tf/r0;
    sol = bvp4c(@max_rad_orbit_odes, @max_rad_orbit_bcs, solinit, option);
    zp = deval(sol, tau);
    rNewt = z(1,end)*r0;
    rNewtp = zp(1,end)*r0;
    rNewtm = zm(1,end)*r0;
    numdaysNewt = numdays;
    numdaysNewtp = numdaysp;
    numdaysNewtm = numdaysm;
```

```
    fNewt = rNewt - targetRadDest;
    fpNewt = (rNewtp - rNewtm)/(numdaysNewtp - numdaysNewtm);
    numdays = numdaysNewt - fNewt/fpNewt;

    % Store solinit data
    solinit.y = z;
    solinit.x = tau;

    % Report when done with iteration
    fprintf("Newton iteration done, r: %10.3f km\n", rNewt);
end

% Solution
sol = bvp4c(@max_rad_orbit_odes, @max_rad_orbit_bcs, solinit, option);

% Evaluate solution at all times
z = deval(sol, tau);

% Extract solutions for each state variable from the matrix Z
rbar_sol = z(1,:);
theta_sol = z(2,:);
ubar_sol = z(3,:);
vbar_sol = z(4,:);
lambda2_sol = z(5,:);
lambda3_sol = z(6,:);
lambda4_sol = z(7,:);
time = t0 + tau.*(tf-t0);

% Plotting trajectory
figure(1)
plot(rbar_sol.*cos(theta_sol)*r0, rbar_sol.*sin(theta_sol)*r0, 'm');
title('Colin Miller: Far-Future Minimum-Time Trajectory to Mars');
xlabel('[km]');
ylabel('[km]');
circ = 0:0.01:2*pi;
grid on
hold on
plot(targetRadDepa*cos(circ), targetRadDepa*sin(circ), 'b');
```

```
plot(targetRadDest*cos(circ), targetRadDest*sin(circ), 'r');
axis equal
legend("Transfer", "Almost Earth", "Almost Mars", "Location", "Best");

% Plotting control history
fprintf("The maximum radius is %15.4f km\n", rbar_sol(1,end)*r0);
fprintf("The transit time is %15.4f days\n", time(end)/3600/24);
figure(2)
plot(time, atan2(lambda3_sol, lambda4_sol)*180/pi);
title("Colin Miller: Far-Future Control History of Orbit Trajectory to Mars");
xlabel("Time (s)");
ylabel("Angle (deg)");
grid on
```

Equations of motion subfunction:

```
function dX_dtau = max_rad_orbit_odes(tau, X)
%%%%%%%%%%%%%%%%%%%%%%%%%%%%%%%%%%%%%%%%%%%%%%%%%%%%%%%%%%%%%%%%%%%%%%%%%%%%%%%
% ODEs for maximizing orbit radius given constant thrust
%
%%%%%%%%%%%%%%%%%%%%%%%%%%%%%%%%%%%%%%%%%%%%%%%%%%%%%%%%%%%%%%%%%%%%%%%%%%%%%%%

global eta accbar nu

rbardot = X(3)*eta;                                    % X(1) = rbar
thetadot = X(4)/X(1)*eta;                              % X(2) = theta
ubardot = (X(4)^2/X(1) - 1/X(1)^2)*eta + accbar*...
          -X(6)/sqrt(nu*X(6)^2+X(7)^2);                   % X(3) = ubar
vbardot = -X(3)*X(4)/X(1)*eta + accbar*...
          -X(7)/sqrt(nu*X(6)^2+X(7)^2);                   % X(4) = vbar
lambdarbardot = X(6)*(X(4)^2/X(1)^2 - 2/X(1)^3)*eta -...
                X(7)*X(3)*X(4)/X(1)^2*eta;             % X(5) = lambdarbar
lambdaubardot = -X(5)*eta + X(7)*X(4)/X(1)*eta;        % X(6) = lambdaubar
lambdavbardot = -X(6)*2*X(4)/X(1)*eta + X(7)*X(3)/X(1)*eta;   % X(7) = lambdavbar

% Non-dimensionalize

dX_dtau = [rbardot; thetadot; ubardot; vbardot; lambdarbardot; lambdaubardot;...
    lambdavbardot];
return
```

Boundary Conditions subfunction:

```
function PSI = max_rad_orbit_bcs(Y0, Yf)

%%%%%%%%%%%%%%%%%%%%%%%%%%%%%%%%%%%%%%%%%%%%%%%%%%%%%%%%%%%%%%%%%%%%%%%%%%%%
% Boundary condition function for the flat-Earth Optimal Ascent Problem
%%%%%%%%%%%%%%%%%%%%%%%%%%%%%%%%%%%%%%%%%%%%%%%%%%%%%%%%%%%%%%%%%%%%%%%%%%%%

global rbar0 theta0 ubar0 vbar0 ubarf Hf m0 mdot tf thetaf

PSI = [Y0(1) - rbar0;
       Y0(2) - theta0;
       Y0(3) - ubar0;
       Y0(4) - vbar0;
       Yf(3) - ubarf;
       Yf(4) - sqrt(1/Yf(1));
       -Yf(5) + 1/2*Yf(7)/Yf(1)^(3/2) + Hf];

return
```

References

[1] Longuski, J. M., Guzman, J. J., and Prussing, J. E., *Optimal Control with Aerospace Applications*, 1st ed., Springer, New York, 2014, p. 235-239.

[2] Bate, R. R., Mueller D. D., White, J. E., *Fundamentals of Astrodynamics*, 1st ed., Dover, New York, 2016, p. 163-166.

[3] Corey, J. S. A. *Leviathan Wakes*, 1st ed., Orbit, 2011, p. 19, 364.

[4] Wang, X., "Solving optimal control problems with MATLAB - Indirect methods," University of California Irvine.

[5] How, J. P., "Principles of Optimal Control," *MIT Open Courseware*, Lecture 1, MIT, Cambridge, Massachusetts, 2008.

[6] Williams, D. R., "Planetary Fact Sheet - Metric," *NSSDCA*, NASA Goddard Space Flight Center, Greenbelt, Maryland, 2019.

[7] "Perseverance Rover, Mission Timeline - Cruise," URL: https://mars.nasa.gov/mars2020/timeline/cruise/

[8] Gooding, R. H, "A New Procedure for Orbit Determination Based on Three Lines of Sight (Angles Only)," Defence Research Agency, Farnborough, Hampshire, UK, April 1993.